

SURFACE COMPOSITION AND TOPOGRAPHY OF FAST-FIRED RAW GLAZES

Linda Fröberg, Stina Vane-Tempest and Leena Hupa

Åbo Akademi University, Process Chemistry Centre
Turku, Finland

ABSTRACT

In this work the development of the phase composition of some fast-fired raw glazes is discussed. The glazes were fired on floor tiles in an industrial furnace. The glaze surfaces were studied by SEM/EDXA, XRD and AFM. The sintering reactions were estimated from the sintering curves recorded by HSM. SEM-images of the glaze samples quenched from interrupted HSM measurements were used to further interpret the sintering curves. The raw glazes are likely to be sensitive to variations in the temperature if fast-fired just above 1200 °C. In the final glaze surface this is seen as differences in the relative amount and size of the crystals originating either from the raw material mixture or formed during the firing. The results indicate that high contents of quartz in the raw material mixture usually give some residual quartz in the glaze surface. These quartz particles are the main reason for large variations in surface roughness. During the firing diopside, wollastonite and pseudowollastonite crystals giving the surface a mat appearance are formed. All the crystal types lead to a pronounced micro-roughness of the surface if present as groupings of tiny crystals.

1. INTRODUCTION

The goal of this work is to study the development of the surface structure of raw glazed tile surfaces during fast firing. Raw glazes are often used on ceramics fired at peak temperatures higher than 1200 °C. In a traditional firing process the glaze is well matured consisting of a glassy phase and one or more crystalline phases developed during the cooling cycle in a desired manner. In modern manufacture of glazed floor tiles and swimming-pool tiles a fast firing process is often utilized. The close-to-zero porosity requirement for the tiles is achieved by using a firing temperature just above 1200 °C. Thus the utilisation of the raw glazes is a lucrative alternative to fritted glaze compositions in floor tiles. The raw material composition of the fast-fired glazes should be carefully selected to ensure that a desired surface composition and topography are developed despite of the short firing time.

Hot Stage Microscopy (HSM) has been widely used to study the sintering process of fritted and raw glazes^[1-9]. The mat appearance of a fast-fired glaze can be due to crystals originating both from residual crystalline raw materials and crystals formed during the firing cycle. In fast-fired raw glazes non-reacted wollastonite crystals have been observed when using wollastonite mineral as a raw material for calcium oxide. These wollastonite crystals were found to decrease the chemical resistance of the surface^[10]. The origin and the chemical composition of the crystalline phases are likely to affect the chemical resistance of the surface. The chemical resistance of the experimental tile surfaces in this work are reported in another study^[11].

Atomic Force Microscopy (AFM) has recently been used to image the topography and roughness of ceramic surfaces in nanometer scale. Most examples are found among advanced ceramics, functional surfaces and glass surfaces. AFM has been used to study also glazed surfaces with a high gloss^[12, 13, 14]. Mat floor tiles have usually a surface roughness on micron-scale. This makes the topography measurement of tiles surfaces with AFM laborious. Another disadvantage is that the surface area measured with AFM is very small and does not often be representative for whole the surface. However, the boundary characteristics of a single crystal in the surface of the glassy phase can be of interest for evaluating the corrosion and soiling behaviour of the glaze.

2. EXPERIMENTAL

In this work the firing properties and the development of the surface structure of four glazes with gloss values between 20 and 80 were studied. The glaze compositions were selected to describe the development of the surface properties rather than to as such be commercially attractive new alternative glaze compositions.

The glazes were ball milled of commercial grade raw materials. The glaze suspensions were applied on green floor tiles in a waterfall-coating process. The tiles were fast-fired in an industrial furnace with a total firing cycle of approximately 1 hour and a peak temperature of 1215 °C. The raw material and the oxide composition of the glazes are given in Table 1. The gloss of each glaze is also given in the table.

Raw Material Composition (wt-%)	A1	A2	A3	A4
Kaolin	8.0	8.0	8.0	8.0
Feldspar	26.0	26.2	27.2	48.0
Dolomite	15.0	15.0	15.4	7.4
Whiting	17.8	17.7	0	22.1
Corundum	13.0	0.3	0.6	3.0
Quartz	20.2	32.8	48.8	11.5
Oxide composition (wt-%)				
Na ₂ O	1.8	1.8	1.7	3.2
K ₂ O	2.2	2.3	2.2	3.8
MgO	4.0	4.0	3.7	2.0
CaO	17.5	17.4	5.4	17.5
Al ₂ O ₃	25.0	10.1	9.9	17.5
SiO ₂	49.5	64.5	77.1	56.0
Gloss	34.1	42.5	15.2	82.4

Table 1. Raw material and oxide composition of the experimental glazes in wt-%. The gloss value of the glazes fast-fired to 1215 °C is also given.

The sintering behaviour of the glazes was measured with HSM (Misura 3.0 by Expert System). The dry raw material mixtures of the raw glazes were pressed into cylindrical samples (height 3.0 mm and diameter 2.0 mm) and heated at a constant rate of 5 °C/min up to 1400 °C. The samples were automatically imaged by a video camera at every 5 °C increase in temperature. The changes in the height of the image were used to compare the firing behaviour of the glazes. The proceeding of the sintering reactions was further studied by heating the samples to several temperatures within the sintering range, i.e. 1100 – 1250 °C after which the samples were cooled by using the maximum cooling rate of the HSM-furnace. SEM-images of the cooled samples were used to interpret the different stages of the sintering curves.

The surface composition of the glazed tiles was determined by SEM/EDXA (LEO 1530) and X-ray analysis (X'pert by Philips). The influence of the crystalline phases on the topography and surface roughness of the glazes was measured with AFM (JEOL JSPM-4200).

3. RESULTS AND DISCUSSION

SEM-images of the surfaces in Figure 1 show that all the experimental glazes have crystals in their surfaces when fast-fired to 1215 °C. SEM-EDX analyses of the different phases are listed in Table 2. The identification of the crystalline phases according to XRD of the surfaces is given in Figure 3 and Table 2.

Basically four different crystal types were observed in the surfaces. The main crystal type in Glaze A1 is a plate-like diopside crystal with a length varying from roughly 2 to 10 µm. In the SEM-image the colour of the diopside crystals is very close to the colour of the glassy phase. Diopside crystals were also identified in Glaze A2. Besides diopside crystals Glaze A2 contains white needle-like wollastonite crystals. In Glaze A3 the main crystalline phase is quartz shown as dark grey spots in the SEM-image. Glaze A3 is of poor quality with several cracks in the surface. Close to the

quartz crystals, but also in the glassy phase very small light coloured diopside crystal groups can be seen. Quartz crystals can be identified in all the other glazes too, but only in Glaze A3 the borders between the quartz particles and the glassy phase are distinct. Glaze A4 contains also a few white, hexagonal crystals. These crystals were identified as pseudowollastonite.

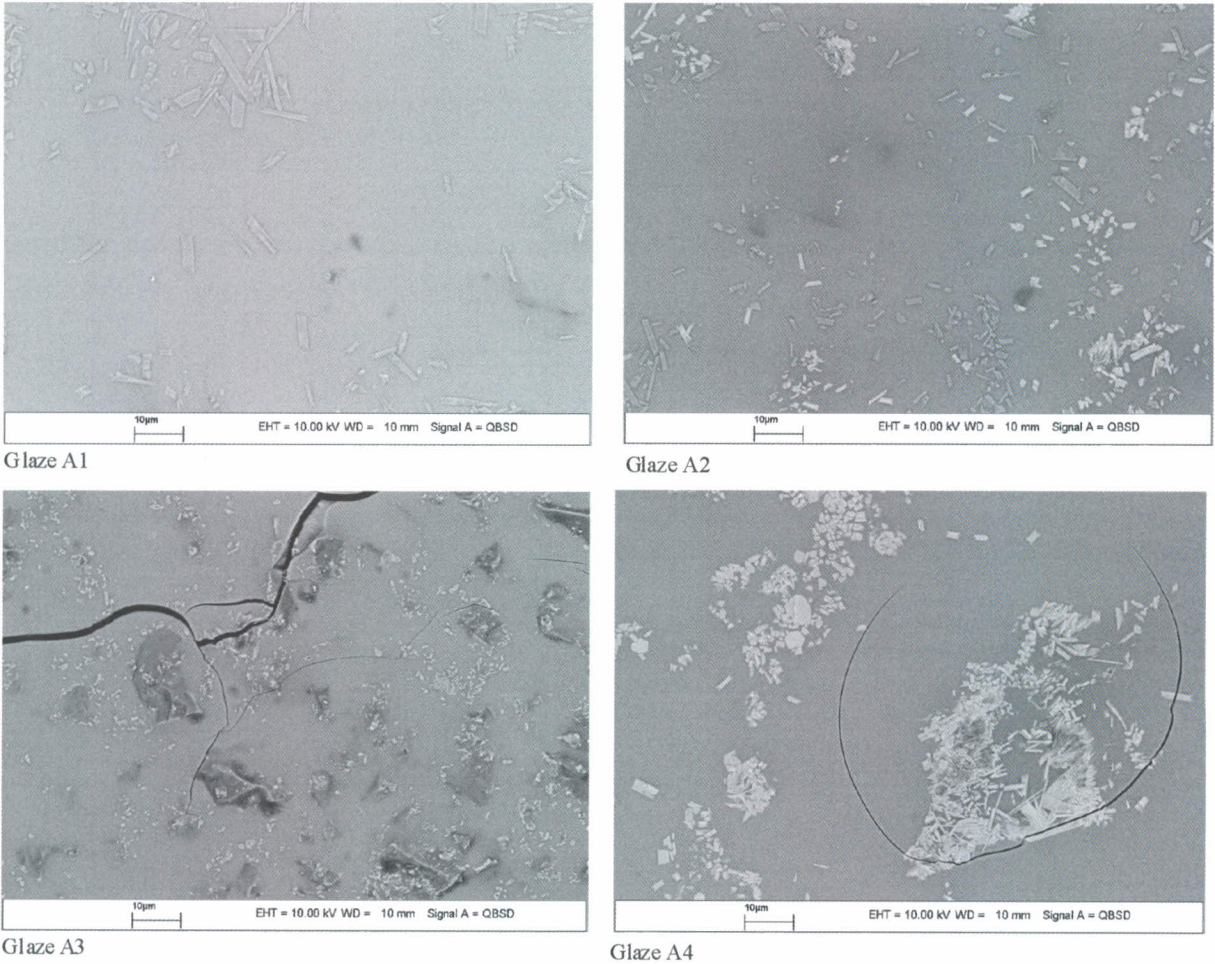


Figure 1. SEM-images of the experimental glazes showing the crystalline phases in the surfaces.

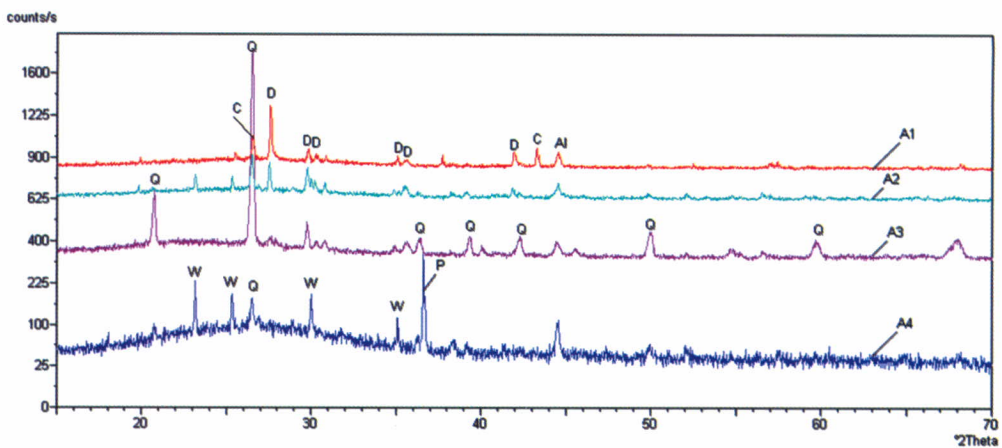


Figure 3. XRD-diffractograms for the experimental glazes showing the main peaks and corresponding crystal phases. The typical peaks for the different crystalline phases are marked. D = Diopside, C = Corundum, Al = Aluminium, Q = Quartz, W = Wollastonite and P = Pseudowollastonite.

Phase (XRD) and description (Figure 1)	A1	A2	A3	A4
Diopside plate-like, light grey	MgO 18	MgO 17	MgO 15	
	CaO 24	CaO 25	CaO 16	
	SiO ₂ 55	SiO ₂ 54	SiO ₂ 60	
	Al ₂ O ₃ 2	Al ₂ O ₃ 3	Al ₂ O ₃ 6	
Diopside light grey nuclei	MgO 5	MgO 15	MgO 4	
	CaO 17	CaO 14	CaO 9	
	SiO ₂ 57	SiO ₂ 61	SiO ₂ 77	
	Al ₂ O ₃ 14	Al ₂ O ₃ 13	Al ₂ O ₃ 6	
Wollastonite Needlelike, white		CaO 33		CaO 40
		SiO ₂ 62		SiO ₂ 50
		Al ₂ O ₃ 2		Al ₂ O ₃ 1
Pseudowollastonite Hexagonal, white				CaO 46
				SiO ₂ 52
Quartz dark grey	SiO ₂ 90	SiO ₂ 91	SiO ₂ 93	SiO ₂ 92
	Al ₂ O ₃ 2	Al ₂ O ₃ 3	Al ₂ O ₃ 1	Al ₂ O ₃ 0
Glassy phase	Na ₂ O 2	Na ₂ O 2	Na ₂ O 2	Na ₂ O 3
	K ₂ O 3	K ₂ O 2	K ₂ O 3	K ₂ O 4
	MgO 4	MgO 2	MgO 5	MgO 2
	CaO 17	CaO 15	CaO 7	CaO 15
	Al ₂ O ₃ 15	Al ₂ O ₃ 11	Al ₂ O ₃ 16	Al ₂ O ₃ 15
	SiO ₂ 58	SiO ₂ 66	SiO ₂ 67	SiO ₂ 59

Table 2. Average chemical composition of the crystals and the glassy phase according to SEM-EDXA in wt-% for the main components. The identification of the crystal phases is based on XRD-results given in Figure 3.

Out of the crystalline phases detected only quartz is also present in the raw material mixtures, all the other crystal phases are formed in the reactions between the raw materials. The influence of the crystalline phases in the surface topography was studied with AFM. Figure 4 shows some examples of the boundary characteristics of single crystals and crystal groups in the surfaces of the experimental glazes.

The surface of the plate-like diopside crystals is relatively smooth. The crystals are oriented along the glaze surface (c.f. Figure 4a). The boundary between the crystals and the glassy phase forms clear thresholds in the surface, which might cause soiling problems. Wollastonite crystals have tubular form, Figure 4b. The outer crystal surface is clearly higher than the main glassy surface, Figure 4b. Quartz crystals and also larger aggregations of the other crystals clearly break the glaze surface and cause distinct differences in the surface topography. Figure 4d shows an example of the surface with several tiny wollastonite crystals and one pseudowollastonite crystal surrounding the residual quartz particle. Figure 4c shows a typical surface topography close to a large non-dissolved quartz particle. All the crystal types identified increase the roughness of the surfaces. The average roughness of the surfaces close to the different crystals is given in Table 3. Roughness Average, Ra is based on the average centreline of a surface, and describes the average height or depth of the peaks above and below the centreline. Roughness Root Mean Squared, RMS is sensitive to the peaks and valleys on a surface and takes into consideration also the value of extreme peaks. Rz is the average maximum height

of the surface profile. It should be pointed out that the total roughness of the experimental surfaces is increased by cracks and larger quartz particles especially in Glaze A3.

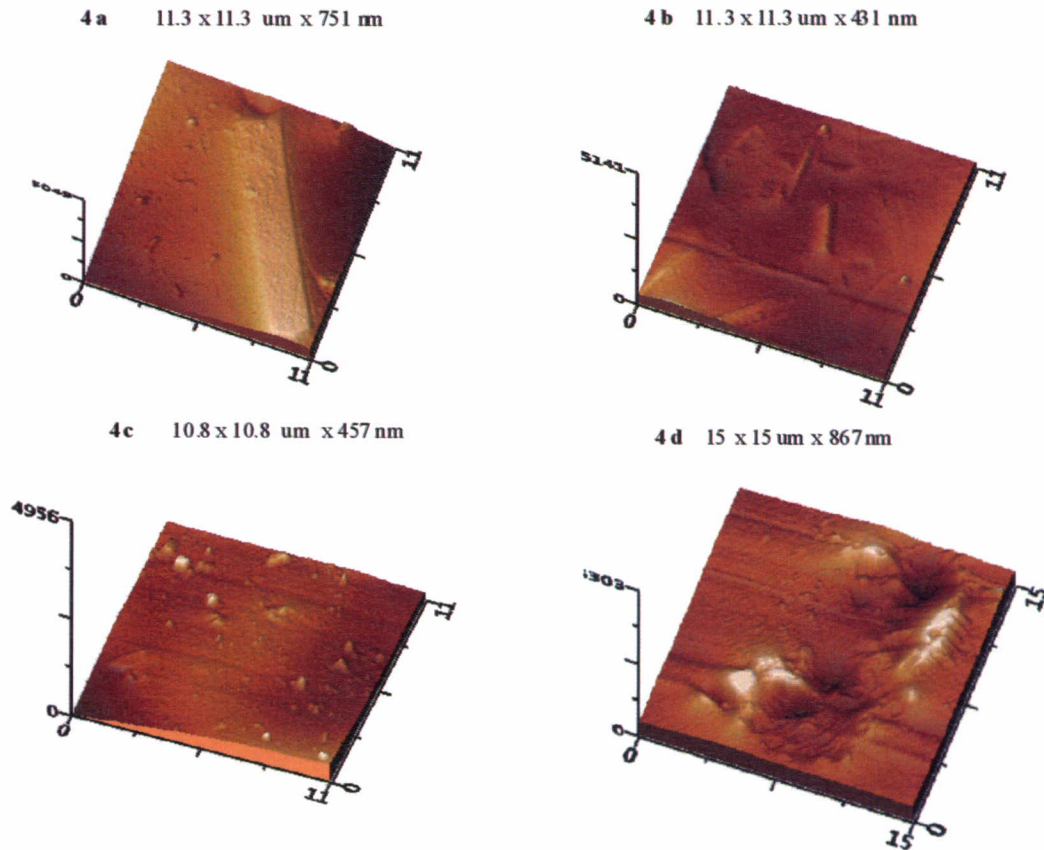


Figure 4. AFM-images showing the boundaries of different crystals: a) diopside, found in glaze A1, b) wollastonite and diopside, found in glaze A2, c) non-reacted small quartz crystals, Glaze A3 and d) quartz and tiny diopside crystals, found in glaze A4. For each figure the scanned area and the maximum height difference in the figure are shown.

Glaze	Size of the analysed area	Ra	RMS	Rz
A1	11.3 x 11.3 μm	116 nm	145 nm	709 nm
A2	10.7 x 10.7 μm	46.9 nm	60.5 nm	376 nm
A3	10.8 x 10.8 μm	37.8 nm	48.8 nm	360 nm
A4	15.0 x 15.0 μm	69.6 nm	96.5 nm	729 nm

Table 3. Surface profile parameters close to the typical crystalline phases in the experimental glazes (c.f. Figure 4).

The sintering of the samples during constant heating in HSM is given in Figure 5. The glazes start to sinter roughly at the same temperature, 1100 °C. SEM-images of these four glazes quenched from 1100 °C in Figure 6 show some neck-growth but the mixtures consist mostly of separate raw material particles.

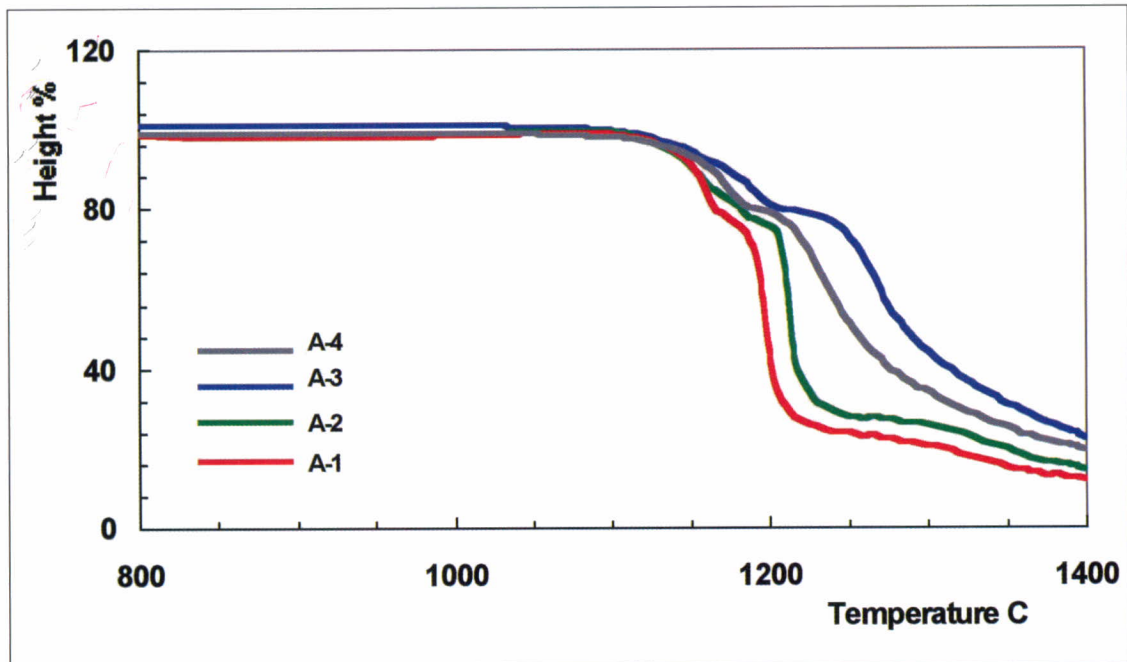


Figure 5. Sintering of the glazes according to HSM.

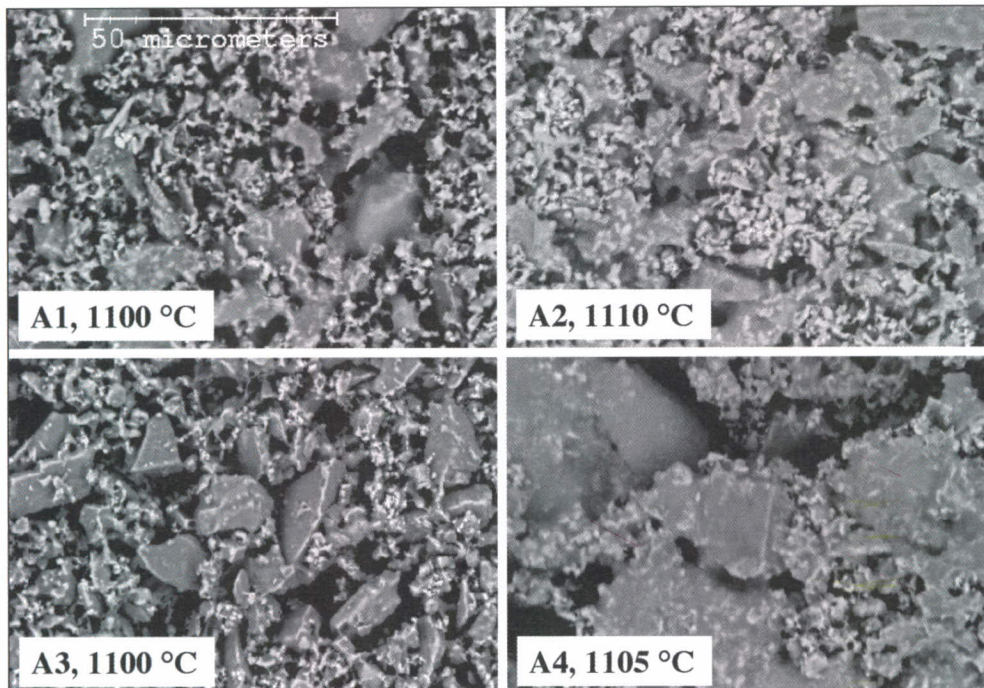


Figure 6. SEM-image of the glazes heated in HSM and quenched from a temperature corresponding to the commencement of the shrinkage of the sample.

As the temperature is increased the height of the samples decreases with different slopes depending on the main reaction type in the mixture. The height of Glaze A1 decreases steeply between 1100 and 1160 °C, and further between roughly 1190 and 1210 °C. In the SEM-image of the sample sintered at 1150 °C, i.e. at the temperature range for the first steep height decrease, separate raw material particles can still be observed.

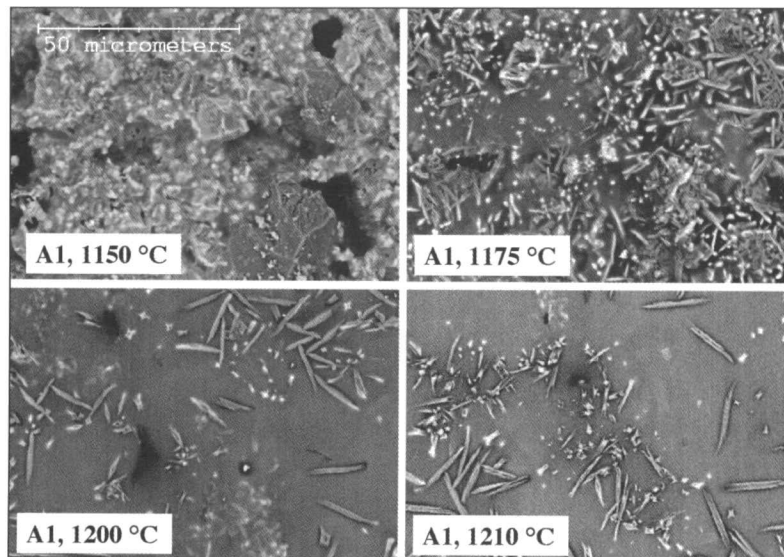


Figure 7. SEM-images of Glaze A1 heated in HSM and quenched from the temperatures indicated.

A SEM-image of the sample within the mild height decrease, at 1175 °C, shows that the particles have grown together and the crystallisation of diopside has started. At higher temperatures the diopside crystals start to dissolve in the melt. Some diopside crystals are still present in a sample quenched from 1250 °C.

The height of the sample of Glaze A2 decreases steadily between 1100 and 1200 °C, and steeply between 1200 and 1220 °C. The SEM-images for this glaze quenched from different temperatures show that the sintering is incomplete still at 1175 °C, but the crystal formation has started on the particle surfaces (c.f. Figure 8). At 1185 °C the sintering is almost complete and the crystals can be clearly seen. At 1215 °C three different crystal types are observed. According to SEM/EDXA these crystals correspond to quartz (dark particles), diopside (small white particles) and wollastonite (featherlike crystals). In a sample quenched from 1250 °C only a few particles of residual quartz were observed.

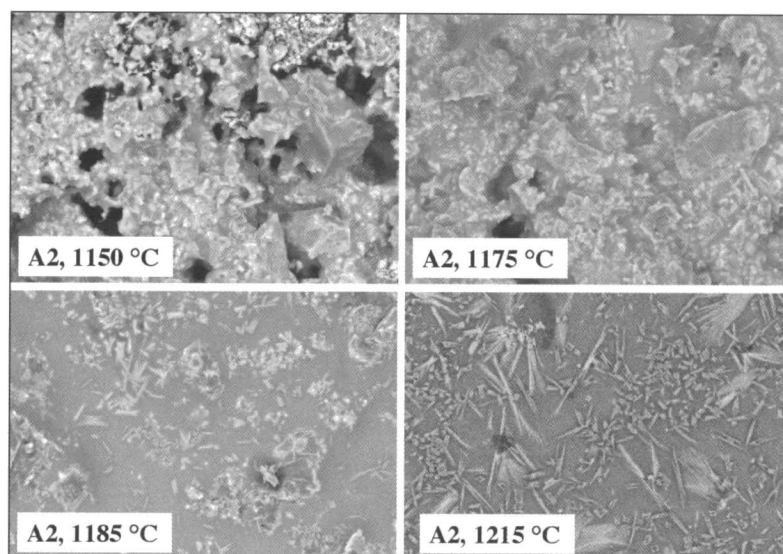


Figure 8. SEM-images of Glaze A2 heated in HSM and quenched from the temperatures indicated.

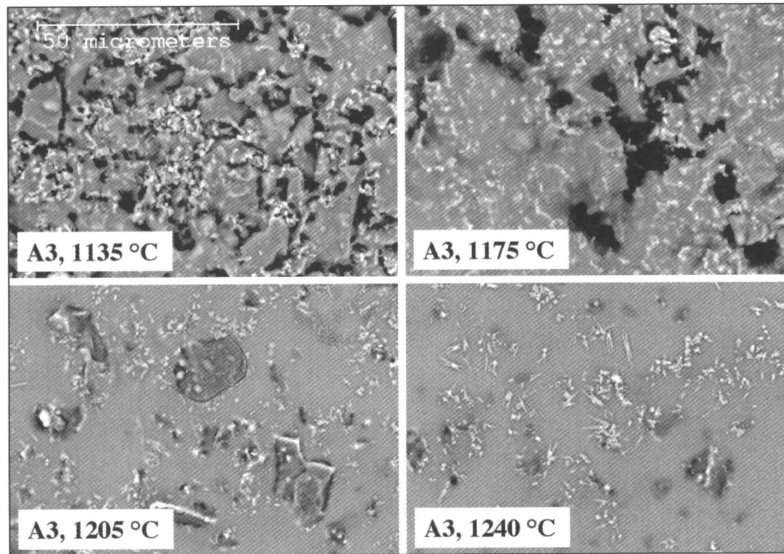


Figure 9. SEM-images of Glaze A3 heated in HSM and quenched from the temperatures indicated.

The sintering curve of Glaze A3 shows a mild decrease of the sample height between 1100 and 1200 °C. The height starts to decrease more pronouncedly again from roughly 1240 °C, but does not level out within the temperature range studied. The SEM-images for the quenched samples given in Figure 9 show the growth of white diopside and wollastonite around the dissolving quartz particles. In a sample quenched from 1280 °C several quartz particles but no other crystals were observed.

The sintering curve of Glaze A4 shows a decrease between 1100 and 1180 °C, and a again one after roughly 1210 °C. Formation of wollastonite crystals around the quartz particles is clearly seen in the glaze already at 1155 °C (Figure 10). At 1195 °C formation of some hexagonal pseudowollastonite crystals can be observed. The few star-shaped crystals might indicate the formation of tridymite. Tridymite was not identified in XRD analysis of Glaze A4. At 1215 °C the amount of pseudowollastonite and tridymite crystals has increased. The wollastonite crystals can be distinguished by their typical featherlike shape. A sample quenched from 1250 °C contains a few quartz particles but no other crystalline phases.

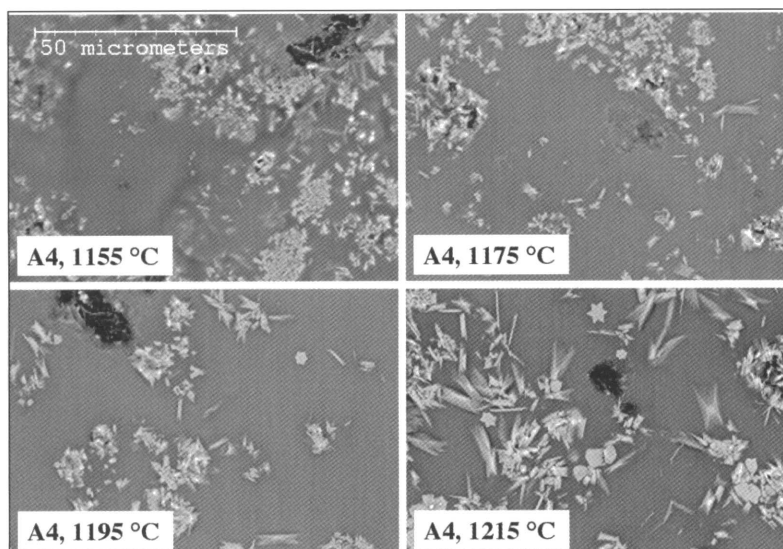


Figure 10. SEM-images of Glaze A4 heated in HSM and quenched from the temperatures indicated.

The SEM-images of the raw-glazes heated with HSM clearly show that the first steady decrease in the sample height correlates with the sintering to close-to-zero densification. In the three first glazes the densification is assumed to depend on the reactions between quartz and the carbonate containing raw materials dolomite and whiting to silicates. The smaller the ratio of carbonates to quartz the milder the slope of the sintering curve. The decrease of the slope of the sintering curve is clearly seen by comparing the glazes A1, A2 and A3 with decreasing carbonates to quartz ratio. The slope for the sintering of Glaze A4 can be explained by its high content of the fluxing component feldspar. It is assumed that the initial sintering of Glaze A4 depends on the reaction between whiting and quartz. Simultaneously also the feldspar gradually melts, and the nucleation of wollastonite close to quartz particles commences. The melt formed by feldspar has a high viscosity thus decreasing the slope of the sintering curve.

After the carbonates have reacted with quartz and feldspar to silicates the nucleation of diopside and wollastonite commences. The crystal growth is assumed to cause the observed changes in the slopes of the sintering curves from more steep to a milder or even a plateau like part. When the slope changes are compared with the SEM-images and XRD-analyses typical crystal growth temperatures can be suggested. The growth of diopside crystal commences from roughly 1160 °C and wollastonite from 1180 °C. In glazes containing both dolomite and whiting the formation and amount of wollastonite is assumed to depend on the free quartz left in the mixture after its reaction with dolomite. However, if the dolomite content is low only wollastonite and pseudowollastonite are formed (Glaze A4).

Pseudowollastonite crystals were observed at roughly 1190 °C in Glaze A4, i.e. the only experimental glaze in which diopside crystals were not identified. Pseudowollastonite is the high-temperature form of wollastonite. The structure modification takes place at around 1200 °C after the impurities from wollastonite crystals have dissolved^[15]. In this work the wollastonite crystals in Glaze A4 have a molar ratio of CaO to SiO₂ closer to the theoretical 1:1 ratio than in Glaze A2. This observation confirms that pseudowollastonite is formed only in glazes with relatively pure wollastonite crystals close to 1200 °C^[15].

When the temperature is increased the crystals start to dissolve in the melt, which is seen as the second steeper slope of the sintering curves. At the firing temperature of 1215 °C the sintering curve of Glaze A1 is levelling out, but the slope of Glaze A2 is very steep. This indicates that the relative amounts of the different phases in Glaze A2 are sensitive to small variations in the firing temperature. Glazes A3 and A4 contain at the firing temperature a high content of non-reacted quartz. In these glazes the ongoing silica dissolution is likely to favour the crystal growth of silica containing crystals. However, only non-dissolved quartz and diopside are identified in the samples fired at roughly 1250 °C. This indicates that diopside and quartz have either a higher liquidus temperature or slower dissolution rate than the two other crystalline phases wollastonite and pseudowollastonite.

4. CONCLUSIONS

The phase composition and the surface structure of fast-fired raw glazes are sensitive to the firing temperature when the peak temperature is close to 1200 °C. At this temperature the dissolution of quartz is seldom complete. The ongoing quartz dissolution strongly affects the crystal growth of diopside and wollastonite. In glazes

with low magnesia content also pseudowollastonite crystals can be formed. All the crystals formed during firing are rather regular and relatively small. The chemical composition of the crystalline and the glassy phases formed during the firing are relevant for the chemical resistance of the fast-fired raw glazes ^[1].

AFM topography measurements show a fairly smooth roughness profile when scanning on the glassy phase, while non-reacted crystalline quartz particles give large height differences in the surface roughness profile. The surface roughness caused by diopside, wollastonite and pseudowollastonite depends on the size of the crystals. Diopside crystals have a flat surface but the borders of the crystals form typical thresholds in the glaze. Wollastonite crystals also clearly rise from the glassy surface with their tubular walls. The surface of pseudowollastonite crystals is like diopside smooth. If any of these crystal types is found in groups of several crystals touching each other, the surface micro-roughness is increased. These results are accordant with the commonly known effects of using whiting and dolomite to achieve a satin glaze surface.

5. ACKNOWLEDGEMENTS

This work is a part of the activities at Åbo Akademi Process Chemistry Centre, a National Centre of Excellence nominated by the Academy of Finland. The financial support from the Finnish National Technology Agency (TEKES) Programme Clean Surfaces 2002-2006 and the Graduate School of Materials Research are gratefully acknowledged. The work has also been supported by IDO Bathroom Ltd, Pukkila Oy Ab. Ms Jaana Paananen is thanked for the preparation of the samples, and Dr Kaj Fröberg and Mr Clifford Ekholm for their help with the SEM and XRD analyses.

REFERENCES

- [1] Burzacchini, B., Paganelli, M., Crist, H.G., Examination of Fast-Fired Frits and Glazes Using a Hot Stage Microscope at Different Heating Rates, *Ceram. Eng. Sci. Proc.* 17 (1), (1996) 60.
- [2] Paganelli, M., Understanding the Behaviour of Glazes: New Test Possibilities Using the Automatic Hot Stage Microscope "Misura", *Ind. Ceram.* 17, (1997) 69.
- [3] Aparisi, J., Sánchez, L.F., Amorós, J.L., Escardino, A., Orts, M.J., Mestre, S., Obtaining Smooth, White Floor Tile Glazes from Zirconium-free Frits, *Qualicer 98 Castellon (Spain) G1-65*, (1998).
- [4] Boccaccini, A.R., Hamann, B., *J. Mater. Sci.* 34, (1999) 5419.
- [5] Siligardi, C., D'Arrigo, M.C., Leonelli, C., Sintering Behavior of Glass-Ceramic Frits, *Am. Cer. Soc. Bull.*, 79 (8), (2000) 88.
- [6] Pascual, M.J., Pascual, L., Duran, A., *Phys. Chem. Glasses* 42, (2001) 167.
- [7] Ahmed, M., Earl, D.A., Characterizing Glaze-Melting Behavior via HSM, *Am. Cer. Soc. Bull.*, 81 (3), (2002) 47.
- [8] Kronberg, T., Hupa, L., Fröberg, K., Optimizing of Glaze Properties, *Ceram.Eng.Sci.Proc.* 22(2), (2001) 179.
- [9] Kronberg, T., Hupa, L., Fröberg, K., Modelling of Firing Behaviour of Raw Glazes, *Advances in Science and Technology (Faenza Italy)*, (2003), 34 (*Science for New Technology of Silicate Ceramics*) 55-62.
- [10] Kronberg, T., Hupa, L., Fröberg, K., Durability of Mat Glazes in Hydrochloric Acid Solution, 8th European Ceramic Society Conference and Exhibition, Istanbul 2003, in print.
- [11] Vane-Tempest, S., Fröberg, L., Kronberg, T., Hupa, L., Chemical resistance of fast-fired raw glazes in solutions containing cleaning agents, acids or bases, Submitted for Qualicer 2004.
- [12] Iwasawa, J., Aoshima, T., Ito, M., Ando, M., Surface Analysis of glaze of sanitary ware, *J. of Surface Analysis* 7 (3), (2000) A/38-A/39.
- [13] Prica, M., Atomic Force Microscope as a tool for imaging green and fired ceramic powder compacts, *British Ceramic Transactions* 97 (3), (1998) 126-129.

- [14] Karlsson, S., Iwasa, M., Evaluation of Chemical Corrosion of Tableware Glazes by Atomic Force Microscopy 77 (3), (2000) 12-18.
- [15] Merrit, C.W., West, R.R., Sheheen, A.T., A Study of the Reactions at the Interface of a Glazed Wollastonite Clay-Tile Body, College of Ceramics at Alfred University, Report 246, (1958).